NGD simple explanation and interpretation

Olivier Maurice, Blaise Ravelo, Sébastien Lalléchère

NGD simple explanation and interpretation

Olivier Maurice[1*], Blaise Ravelo[2], Sébastien Lalléchère[1]

[1]AFSCET, Systemic Scientific Society, 75000 Paris, France
[2]NUIST, Nanjing, China
*olivier.maurice@e-nautia.fr, blaise.ravelo@yahoo.fr, sebastien.lallechere@protonmail.com

This article presents some proposals for interpreting negative group delay (NGD) phenomenon through electrical circuitry applications. The main idea comes from the normalization process which seems not innocuous. We first recall basic observations about NGD circuits before listing the fundamental properties of these circuits. Then, the way the normalization step influences the NGD procedure is questioned in terms of energy, concluding to its influence and effect on the NGD measurements. A final discussion is proposed regarding the potential prospects in relation with our explanation.

Introduction

The superluminal and negative group delay (NGD) phenomena [1-17] are the most debated topics by scientist and physicist breakthroughs through centuries. The NGD phenomenon interpretation disturbs the common physical feeling about time causality [8-10]. So, the scientist breakthrough was wondered about information speed. Many discussions were initiated about the possibility to overcome the celerity of light or not. But it seems to us that this is not the problem. To verify the existence of the counterintuitive NGD phenomena, many demonstrations signaling this confirmation have been done [2-16] in different domains. In 1950s, Sommerfeld

and Brillouin [18-20] showed theoretically that in the frequency band of anomalous dispersion, the medium group velocity vg can exceed the vacuum light velocity c and even, can become negative. This last effect was developed by Garrett and McCumber in 1970 [1], who emphasized that in this case, the peak of the output Gaussian pulse can leave this output face of this medium before the input one entering. This prediction was validated firstly, in 1982, by Chu and Wong, in 1985, by Macke and Segard, and several experiments in optics wavelengths [2-3]. Despite the empirical investigation at optical wavelengths, the NGD phenomenon understanding question remains an open debate. The main debated point was the physical significance of the realm quantity evolution, such as signal or information interpretation by interacting with the NGD medium or system. So, the first question is "is there more than one referential in the NGD experiment?". Then what is the physical process leading to the NGD measurements? Then, our question may become "is it possible to keep the NGD effect between any referential?" To deal with to the phenomenological problem, experimentations referring to the mathematical presentation of physical variables such as current, voltage, ... were performed [2-17]. The negative GV (NGV) phenomenon was widely investigated with artificial medium constituted by negative refractive index (NRI) metamaterials $n_g = c/\nu_g$, with c is the speed of light [2-6,15-20]. The negative permittivity and negative permeability-based metamaterial theoretical concept was physically inspired by Veselago in late 1960s [21]. The NRI metamaterial verification was experimented in early 2000s by the teams of Pendry and Smith [23-24]. Then, the NRI concept was also investigated at microwave wavelengths. By analogy between the transfer function of resonant atomic systems and electronic circuits which are based on the operational amplifier in negative feedback, Chiao and his co-worker demonstrated these circuits are capable to generate a NGD [8-10]. Indeed, the NGD can be interpreted by the propagation time [21-25], of the Gaussian pulse peak through the NGD circuit, well matched and downstream cascaded with a vacuum medium is less than that through the last one denoted. In this way, the NGD topology

introduced by the team of Chiao [8-13] is not a good candidate due to the frequency limitation only about some hundreds of kHz. Otherwise, another passive circuit was proposed which can operate up to GHz [14-17]. But, the metamaterial NRI [21-24] is technically limited in terms of applications due to its inherent excessive losses systematically associated to the apparition of a significant NGD. To pass the technical limitation, NGD active topologies susceptible to operate at microwave frequencies were introduced [14-17]. In order to transpose this topology in base band frequencies, different topologies can be elaborated via the innovative NGD theory inspired from linear filter theory [25-31]. Topologies of low-pass [25-28], high-pass [25-26, 29], bandpass [25-26, 30], stop-band [25-26] and all-pass [25-26, 31] NGD circuits were innovatively initiated. It is very interesting to underline that the unfamiliar NGD circuits are promising for very interesting applications which expect approbation from end user companies [32-38]. For example, some applications were proposed to integrate the NGD circuits in communication system performance improvement [32], signal integrity enhancement [33-35], pulse compression [36], and resonance effect reduction for electromagnetic compatibility (EMC) engineering [37-38]. In this work, a proof-of-concept (PoC) constituted by lumped circuit network excited by bi-exponential pulse will be considered. To interpret fundamentally the NGD signal propagation, Lorentz's transformation and Einstein's invariant references are considered. The referential system is based on the assumption that the light speed is an invariant and a limit for dynamic systems. But this is not in contradiction with the NGD when it is looked in its own referential as a static process. Then, it is organized as follows; The next section is consecrated to the characterization of the first order linear physical system generating NGD where frequency- and time-domains analysis of such system allowing to explore its causality is given. Afterwards, we investigate the used NGD circuit. In the following section, we focus on the experimentation validating this proposal topic. It is ended by the discussions mainly concentrating to the application of understudied system. Finally, we draw the conclusion about this work.

A simple experience

Many publications [8-17] have already been done giving examples of simple electronic NGD circuits. But we want here to support our discussion on one of these examples. First major observations can be based on its study.

So, we consider a simple RC circuit described (Fig. 1).

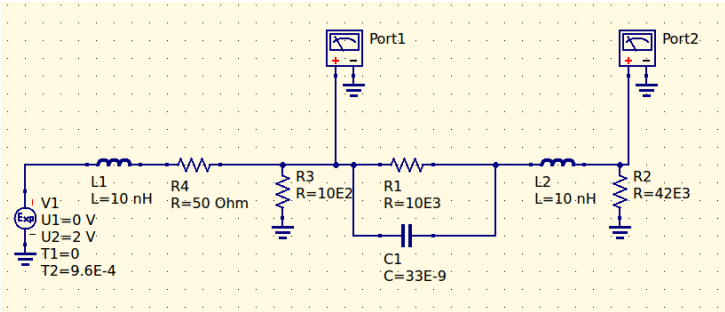

Figure 1: A simple RC circuit

First of all, we attract attention on the fact that this circuit can be strictly realized with real electronic components and facilities. In particular, the signal generator V_1 has its own self impedance R_4. Rather than speaking of the circuit input and output, we voluntary call these classical observation points: ports one and two. We come back on this fundamental notion in the next paragraph. Using any electronic circuit solver we can find the results shown (Fig. 2).

For the moment, as waited, port 2 signal appears with a lower amplitude than port 1 one, and its maximum level is established some time after the maximum level of port 1 voltage. This first example allows us to define as accurate as possible some fundamental facts.

Propagation concept and referential definition

How may we decide if the elements of an experience are in the same referential or not? The question is not so simple as we may think. We must first define what we consider to be a

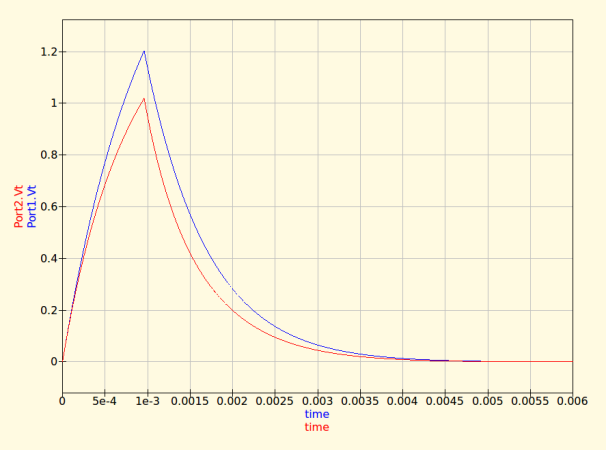

Figure 2: Port1 and 2 voltages

referential. Then when a referential is different from another. And to end, to come back on our first experience.

Referential definition

Once we have defined a configuration space S_0 for a model attached to an experiment, we have implicitly define our referential. If $\{a\}$ is the set of observables of our problem, we make the assumption that all these observables are strictly reachable to measurements. We mean that we can affirm that we don't need any physical modeling to ride up to their real values, except the measurement errors. Or in other words, there are no propagation phenomenon constraining us to consider any delays between the measurements of the various observables.

Let's writing this in the case of the first circuit. It is made of 5 components (s is Laplace's operator): $R_4 + L_1 s, \ldots R_4$, C_1. Each of these components can be represented by a branch in a cellular topology B^1. A graph G is made of nodes, branches and meshes that belong respectively to the spaces N^1, B^1, C^1.

A bijective map $f : b_i \xrightarrow{f} \vec{b}_i$ makes in correspondence each element $b_i \in \mathbb{N}$ of B^1 with the component $\vec{b}_i$ of a vectorial space $\mathbf{B}^1$. Seeing graph G as an oriented and weighted graph, each

branch is associated with a weight $w^i \in \mathbb{C}$. The orientation of one branch i is fixed by $\vec{b}_i$. A flux vector $\vec{w}$ can be defined on this graph through the definition:

$$\vec{w} = w^i \vec{b}_i \tag{1}$$

We create a connectivity C making the link between the branch space and the mesh space $\mathbf{C}^1$. Previously, in our circuit, we can reduce the impedances in parallel R_1, C_1 to a single impedance Laplace's formalism (s is Laplace's operator) $z_1 = R_1/(1 + R_1 C_1 s)$. The circuit is then made of 4 branches:

$$B^1 = \{b_1,\ b_2,\ b_3,\ b_4\} \tag{2}$$

We define C by:

$$w^i = C^i_\mu J^\mu \tag{3}$$

Each component of $\vec{w}$ appears as a linear combination of components J^μ. These components are the components of a vector $\vec{J}$ belonging to the mesh vectorial space. There is also a bijective map $g : c_i \xrightarrow{g} \vec{c}_i$ making the correspondence between each mesh $c_i \in \mathbb{N}$ chosen on the graph ($c_i \in C^1$) and a basic vector of the mesh space $\vec{c}_\mu$. The components $J^\mu \in \mathbb{C}$ are the weights of the mesh flux $\vec{J}$: $\vec{J} = J^\mu \vec{c}_\mu$.

Starting from the graph G and its associated vectorial spaces ($\mathbf{B}^1$, $\mathbf{C}^1$), we can define an exterior product applied on $\mathbf{B}^1$: $\vec{b}_u \wedge \vec{b}_v$. Through this process, an invariant p which is the power for the electrical circuits can be defined writing:

$$p = \frac{1}{2} z_{ab} w^a \wedge w^b \tag{4}$$

The 2-forms can be seen as normalized powers (similar to areas $\in B^2$) and the z_{ab} are the components of a skew symmetric tensor of rank q in a general coordinate system w^α:

$$p = \frac{1}{q!} z_{\alpha\beta\ldots\sigma} w^\alpha \wedge w^\beta \ldots \wedge w^\sigma$$

We could have quite easily verify that $\mathbf{B}^1$ has effectively a structure of vectorial space with the two laws: summation "+" and external product "*". The neutral element is $\vec{0}$ a null branch, and $1\vec{b_i} = \vec{b_i}$.

We can define a dual space $\tilde{\mathbf{B}}_1$ with the elements $\hat{b}^u$ defined by:

$$\hat{b}^u \vec{b}_v = \delta_v^u \tag{5}$$

The covector $\hat{e} = e_u \hat{b}^u$ is in relation with the invariant writing

$$\frac{1}{2} e_u \wedge w^u = p$$

This leads to:

$$e_\mu = z_{\mu\nu} w^\nu \tag{6}$$

$e_\mu \in \mathbb{C}$ can be called a force and seen as a source for the fluxes w^i. But our previous relation must be completed with a scalar ψ, as it remains true when we add such a scalar. It is a gauge function, and the completed equation can be called Kirchhoff's equation:

$$e_\mu = z_{\mu\nu} w^\nu + \psi_\mu \tag{7}$$

By applying the connectivity between the two vectorial spaces and their corresponding in G, we obtain:

$$e_\mu = z_{\mu\nu} C_\alpha^\nu J^\alpha + \psi_\mu \Rightarrow C_\sigma^\mu e_\mu = C_\sigma^\mu z_{\mu\nu} C_\alpha^\nu J^\alpha + C_\sigma^\mu \psi_\mu \tag{8}$$

but as the mesh fluxes do not depend on $\psi \Rightarrow C_\sigma^\mu \psi_\mu = 0$, this leads to:

$$\mathcal{E}_\sigma = \zeta_{\sigma\alpha} J^\alpha \tag{9}$$

As for $\mathbf{B}^1$ we may demonstrate that $\mathbf{C}^1$ has the structure of a vectorial space.

The 2-tensors z or ζ include the branches or meshes properties, i.e. their own impedances and the coupling impedances between branches or meshes.

The dimension of our problem is completely defined by Poincaré's topological relation $D(\mathbf{C}^1) = D(\mathbf{B}^1) - D(\mathbf{N}^1) + D(\mathbf{R}^1)$, where $D()$ is the dimension of each subspace $\mathbf{B}^1$, $\mathbf{N}^1$, $\mathbf{C}^1$ and the number of referential $D(\mathbf{R}^1)$. In the case of our first example, there is 1 referential, so $D(\mathbf{R}^1) = 1$ and there is 1 graph G.

Using the correspondences:

$$\begin{array}{l} b_1 \rightarrow R_4 + L_1 s \\ b_2 \rightarrow R_3 \\ b_3 \rightarrow \frac{R_1}{R_1 C_1 s + 1} + L_2 s \\ b_4 \rightarrow R_2 \end{array}$$

By using also $\zeta_{\sigma\alpha} = C^{\mu}_{\sigma} z_{\mu\nu} C^{\nu}_{\alpha}$, we find:

$$\zeta = \begin{bmatrix} R_4 + L_1 s + R_3 & -R_3 \\ -R_3 & R_3 + R_2 + \frac{R_1}{R_1 C_1 s + 1} + L_2 s \end{bmatrix} \tag{10}$$

The circuit has 4 branches, 2 nodes and so 2 meshes in 1 referential. ζ is a 2×2 tensor. We can separate ζ in two tensors, one g including all the operators which involve the flux derivatives (the inductances for an electrical circuit) and represent the kinetic energy (inertia) of the circuit; and a second Q including all the dissipation or potential energies components (resistances and capacitances).

With this decomposition, the circuit equation becomes:

$$\mathcal{E}_{\sigma} - Q_{\sigma\alpha} J^{\alpha} = g_{\sigma\alpha} s J^{\alpha} \tag{11}$$

$\mathcal{E}_{\sigma}$ contains all the sources of energies (forces) for the circuit.

The circuit can be seen as a construction of both subcircuits $\{b_1,\ b_2\}$ and $\{b_2,\ b_3,\ b_4\}$, themselves constructed from B^1. The connectivity C is an atlas for the manifold $\mathcal{M}$ described by equation (11).

To conclude, our configuration space describes the couple $(G,\ \mathcal{M})$ in the referential $\mathbf{R}^1$.

Note that, as the circuit is completely described with lumped elements, and gives good correlation with the measurements, it is completely coherent with the fact that it exists in an

unique referential, with no time delay functions appearing in Q. We will see further than such interactions involving time delays, cannot be represented with only one referential and need specific time delay functions in Q.

We understand also that there are no input nor output in this circuit, as they exist in the same space-time. That's why we prefer to speak of ports rather than input / output accesses.

About the concept of propagation

Someone may say that "whatever the graph representation, there is a propagation delay over the RLC circuit from port 1 to port 2". Then there are no doubt to write when the measurements re-cut perfectly the computation. The models are only models and any discussion on some hypothetical "reality" is sterile. It is clear that if we increase the source speed, our model will become false, and the NGD effect in the same time will disappear. We come back on these arguments further. So factually, *we consider that there is propagation process* ***each time the function*** $exp\,(-x/vs)$ ***exists in the system equation***.

NGD mechanism and controlled distortion

Now we can add an operational amplifier (op-amp) to make port 2 level reaching port 1 level. This is equivalent to the normalization process often evoked in NGD articles. Adding an operational amplifier, we design the circuit shown in Fig. 3.

which gives the response shown in Fig. 4.

The signal given on Port 3 is distorted in such a way that its front rise exists before the signal front on Port 1. Through this normalization, applied here using an op-amp, some temporal advance can be measured on Port 3 compare with respect to Port 1. But this temporal advance comes from the wanted distortion, and definitely not from any time delay suppression removal. It's like is we have push left the rise and fall edge of the source signal. However there are here

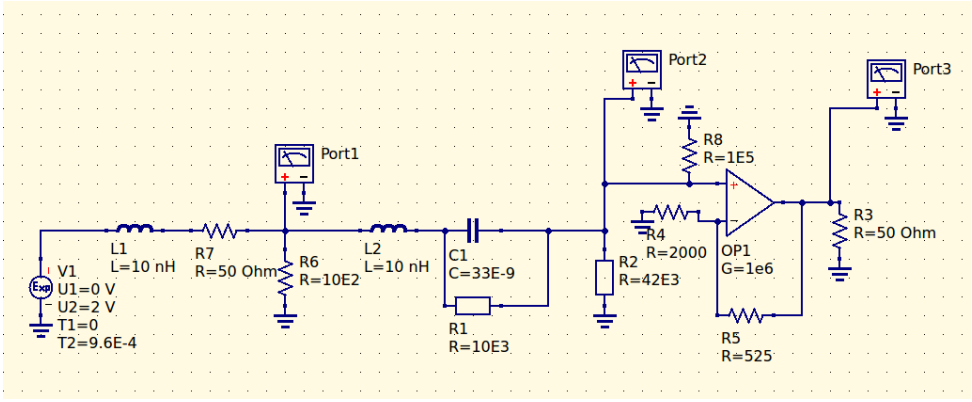

Figure 3: NGD circuit with op-amp

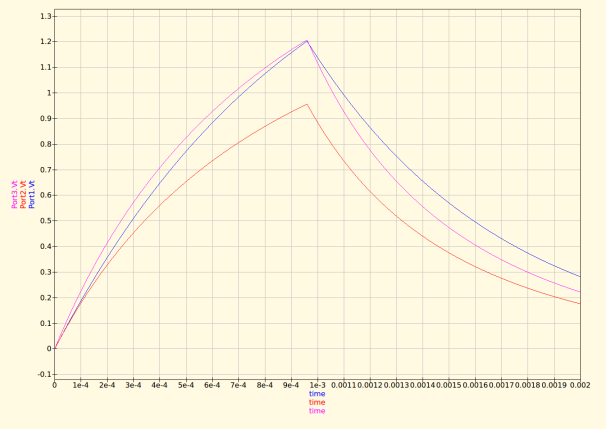

Figure 4: Ports results with op-amp

no time distortion or any particular phenomenon, but through this signal distortion we have really gain some time interval compared to port 1 signal.

To reach this result we need some strict conditions:

1. an active circuit locally on port 2 (the ”normalization circuit”);

2. a source frequency band respecting the NGD band-pass conditions (the source signal must be sufficiently slow compared to the NGD circuit typical time constant).

Propagation speed in the single referential NGD circuit

The Fig. 5 shows the graph extracted from the classical normalized NGD circuit schematic. Note that even if it doesn't appear on the electrical schematic, any mesh must be accompanied with an inductance. That's why the output mesh is associated with L_4 inductance. In the graph each mesh is represented by a square and the shared rectangle on each frontier points out the coupling function between meshes.

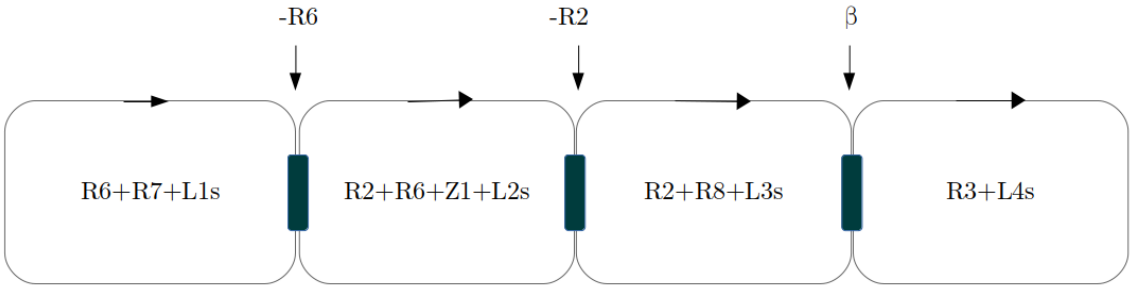

Figure 5: Normalized NGD graph

We can write the equation corresponding to the manifold of this circuit as follows:

$$\frac{1}{s}\left(\mathcal{E}_\mu - Q_{\mu\nu}J^\nu\right) = g_{\mu\nu}J^\nu \tag{12}$$

with:

$$g = \begin{bmatrix} L_1 & 0 & 0 & 0 \\ 0 & L_2 & 0 & 0 \\ 0 & 0 & L_3 & 0 \\ 0 & 0 & 0 & L_4 \end{bmatrix} \tag{13}$$

The right term in equation (12) represents the inertia or in other words a metric, while the left term can be associated with the involved energies (thermal one, losses, sources, etc.). Taking the square root of the left term should lead to a quantity in relation with the speed v (we associate

the system to a fluid for which the energy is expressed by $1/2\rho v^2$). So (with $sq^\alpha = J^\alpha$, $q\alpha$ being the mesh load):

$$v = \sqrt{g_{\mu\nu}\frac{dq^\nu}{dt}\frac{dq^\mu}{dt}} \tag{14}$$

Noting $v^2 = \frac{1}{s}\left(\mathcal{E}_\mu - Q_{\mu\nu}J^\nu\right)$, we come back to the first example to simplify the analysis of this speed in this passive case. We can write its tensors under the form:

$$\mathcal{E} = \begin{bmatrix} e_0 \\ 0 \end{bmatrix} \tag{15}$$

$$Q = \begin{bmatrix} R_0 + \sigma_f & -\sigma_f \\ -\sigma_f & \sigma_f + R_s + z_1 \end{bmatrix} \tag{16}$$

$$g = \begin{bmatrix} L_1 & 0 \\ 0 & L_2 \end{bmatrix} \tag{17}$$

Taking into account the real values of the circuit components and the time variation of the source (for example $L_i s$ becomes negligible) we can approximate the circuit to obtain these results for its fluxes:

$$J^1 = \frac{e_0}{\sigma_f} \tag{18}$$

$$J^2 = \frac{e_0}{z_1 + R_s} \tag{19}$$

We can know write the speed expression in this first case:

$$v = \sqrt{L_1\left(\frac{e_0}{\sigma_f}\right)^2 + L_2\left(\frac{e_0}{z_1 + R_s}\right)^2} \tag{20}$$

Due to the low frequency band of the excitation, we can approximate v with:

$$v = \sqrt{L_1\left(\frac{e_0}{\sigma_f}\right)^2 + L_2\left(\frac{e_0}{R_1 + R_s}\right)^2} \tag{21}$$

Now adding a normalization amplifier with $\beta = (R_1 + R_s)/\sigma_f$, we obtain:

$$v_\beta = \sqrt{L_1\left(\frac{e_0}{\sigma_f}\right)^2 + \beta^2 L_2\left(\frac{e_0}{z_1 + R_s}\right)^2} = \frac{e_0}{\sigma_f}\sqrt{L_1 + L_2} \tag{22}$$

It is clear that $v_\beta > v$ that's why a time advance can be observed **thanks to the normalization process**.

Adding interactions between two referentials

Keeping our first example we can lead two interesting experiments. We add a line between the output of the source and the input of the NGD circuit. We then observe the voltage curve for two line length values: 1 and 10 kilometers. These lengths remains relatively short compared to the signal speed. Remember that the rise time is 0.96 ms. Thinking to a round trip defined by $2r/c = 0.96$ ms, we find a length r equal to 144 kilometers! We understand that our line of some kilometers long seems very short at this scale. We will see on this new example that the ratio between the line length and the signal speed is another key-point to understand the NGD phenomenon.

adding a line before the NGD circuit

Fig. 6 shows the circuit equipped with a line of 1 km. The line is matched on its output and after we find the same circuit as previously. This new structure is made of two parts: a first circuit before the line and a second one after the line. These two circuits are connected by the line which is a delay function.

The physical model of a line which is a guided wave system was found by Branin, based on the line theory and then included in the ATR formalism. Branin's equations applied with an input impedance R_1, an output impedance R_2 and a line of length x with a propagation speed c and a characteristic impedance z_c are:

$$\begin{cases} e_1 = (z_c + R_1)J^1 + (R_2 - z_c)\, e^{-\tau s} J^2 \\ e_1 e^{-\tau s} = (R_1 - z_c)\, e^{-\tau s} J^1 + (z_c + R_2)J^2 \end{cases} \tag{23}$$

Here appears clearly the delay functions, both in the source covector or in the impedance tensor. It means that a time delay exists between the input of the line and the output of the line.

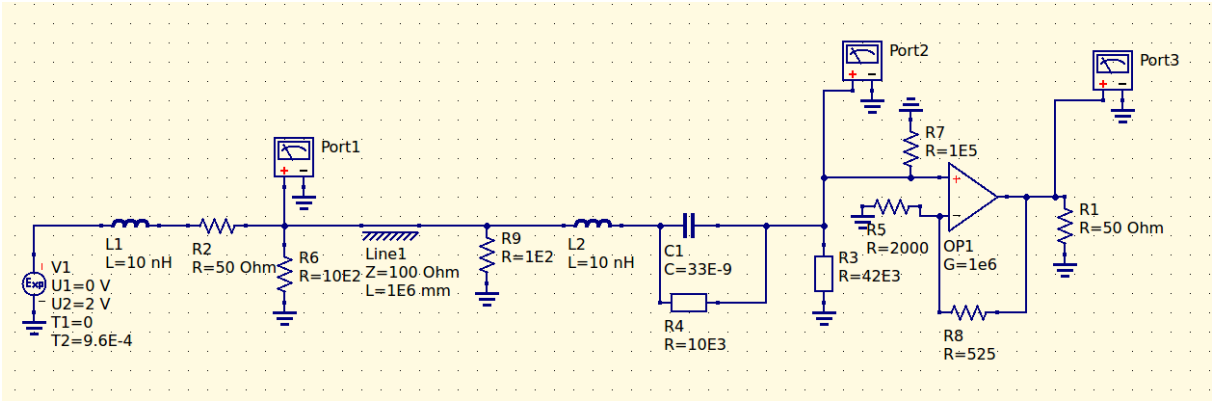

Figure 6: Adding a line to the NGD circuit

Noting $R' = R_2R_6/(R_2 + R_6)$ the impedance tensor of this new circuit is given by:

$$Q = \begin{bmatrix} R' + z_c & 0 & 0 & 0 & 0 \\ 0 & R_9 + z_c & -R_9 & 0 & 0 \\ 0 & -R_9 & R_9 + z_1 + R_3 & -R_3 & 0 \\ 0 & 0 & -R_3 & R_3 + R_7 & \beta \\ 0 & 0 & 0 & \beta & R_s + R_1 \end{bmatrix} \tag{24}$$

The metric being:

$$g = \begin{bmatrix} L_1 s & (R_2 - z_c)e^{-\tau s} & 0 & 0 & 0 \\ (R' - z_c)e^{-\tau s} & L_2 s & 0 & 0 & 0 \\ 0 & 0 & L_3 s & 0 & 0 \\ 0 & 0 & 0 & L_4 s & 0 \\ 0 & 0 & 0 & 0 & L_5 s \end{bmatrix} \tag{25}$$

$\tau = x/c$ is the line time constant.

Fig. 7 shows the graph of the circuit (each mesh having two branches). We clearly see the delayed interaction between port 1 frontier and port 2 frontier. The graph has 7 nodes, 10 branches and 2 referentials. It needs 5 meshes. Due to the fact that a time propagation delay exists between meshes 1 and 2, each network on each side of this propagation zone cannot explicitly know what's happen in the opposite network until it receives its signal. The delay function implies that each world on each side of the propagation belongs to a different referential. This is clearly pointed out by Poincaré's relation $B^1 - N^1 + R^1 = C^1$. In this new problem, we have two different referentials.

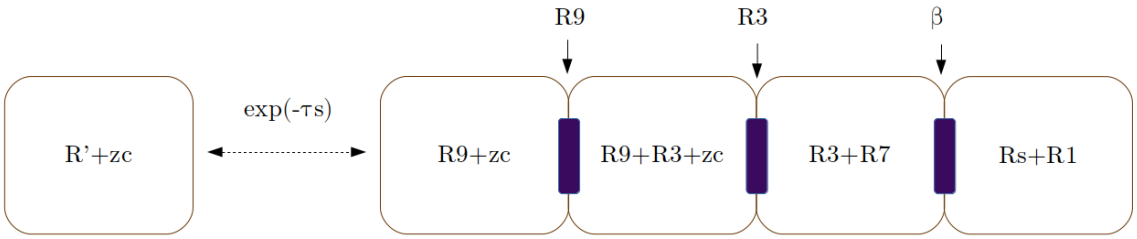

Figure 7: NGD with line graph

If we sent an extremely short pulse as source. The time derivative of this pulse becomes extremely tall. All the other terms seem small compared to this value. We can approximate our problem to the equation $\mathcal{E}_\mu = g_{\mu\nu}J^\nu$. The problem remains the same if we reduce the metric to its two first terms:

$$g = \begin{bmatrix} L_1 s & (R_2 - z_c)e^{-\tau s} \\ (R' - z_c)e^{-\tau s} & L_2 s \end{bmatrix} \tag{26}$$

The current (output flux) on the line output is given by ($\beta_{12} = (R_2 - z_c),\ \beta_{21} = (R' - z_c)$):

$$J^2 = -\frac{\beta_{21}\delta e^{-\tau s}}{L_1 L_2 s^2 - \beta_{12}\beta_{21}e^{-2\tau s}} \tag{27}$$

δ being the input pulse. If $s \to \infty$, the output current tends to:

$$J^2 = -\frac{\beta_{21}\delta e^{-\tau s}}{L_1 L_2 s^2} \tag{28}$$

because the second term of the denominator is negligible, even if delayed. If $s \to 0$, the output becomes (keeping Q very small):

$$J^2 \to \frac{\delta}{\beta_{12}} e^{2\tau s} \tag{29}$$

and $exp(2\tau s) \to 1$. When the frequency tends to zero, the propagation delay tends to be zero also. For a temporal signal covering all frequencies from the lower ones to the higher ones, the low frequencies will propagate faster than the high frequencies, even arrive with zero delay. But when we compute the Spectrum of a temporal signal, as the temporal domain is the dual of the

harmonic domain, globally $t = 1/f$. The higher the frequencies, the smaller the time duration. It means that the high frequencies appear first in the time signal instantaneous spectrum. In other word, the high frequency components are contained in the rise front of the temporal signal. How all this will be translate in our NGD circuit. We have to recall two fundamental results about Coulomb's gauge and Fourier's transformation.

Before to aboard these notions you can take a look to the results of the NGD circuit with line Fig. 8 and to the zoom applied on the first instants Fig. 9. This is synthesized Fig.10.

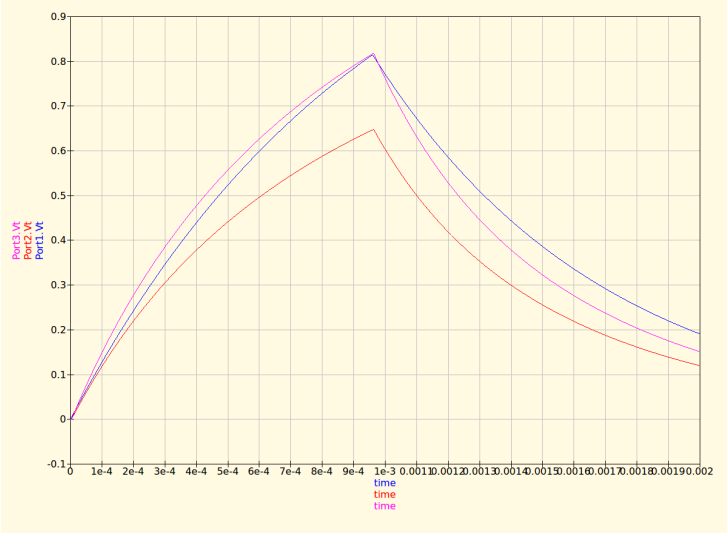

Figure 8: Result NGD with line

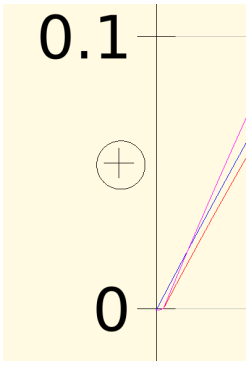

Figure 9: Zoom on the first moments

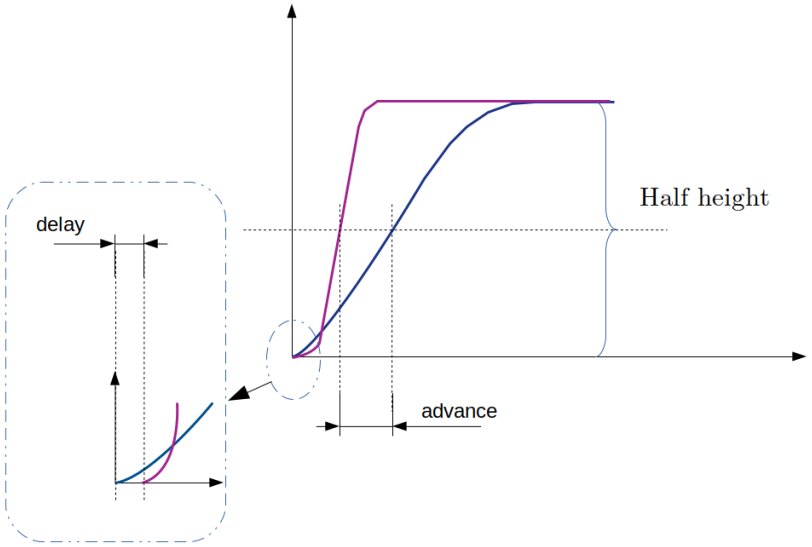

Figure 10: Synthesis NGD with line

Coulomb's gauge behavior in time

In the Coulomb's gauge we chose: $\vec{\nabla} \cdot \vec{A} = 0$, which leads to:

$$\nabla^2 V = -\frac{\rho}{\epsilon_0} \tag{30}$$

While the vector potential is defined by:

$$\frac{1}{c^2}\frac{\partial^2 \vec{A}}{\partial t^2} - \nabla^2 \vec{A} = \mu_0 \vec{J} - \frac{1}{c^2}\frac{\partial}{\partial t}\nabla \vec{V} \tag{31}$$

Quoting Martin and Rothen [39]: "in all space point, V change instantaneously when ρ changes. There is not here contradiction with the theory of relativity because only the electromagnetic field is limited in its propagation speed. Equation (31) is a propagation equation with source. This is it which describes the radiation and which corresponds to the field dynamic degrees of freedom".

In Coulomb's gauge, also called "transverse gauge", the potential vector is transverse to the propagation line. The scalar potential is longitudinal. The coulomb's gauge gives implicitly the

transverse and longitudinal components of the field. We will understand speaking of Fourier's transformation that only the transverse part is submitted to the relativity rule.

Fourier's transformation and DC component

Fourier's transformation change a temporal description of a signal in a frequency description. What is remarkable is that the average component A_0 gives the 0 hertz component, and is in relation with the temporal average value of the signal:

$$A_0 = \frac{1}{T}\int_T dt f(t) \tag{32}$$

It is always possible to compute all the Fourier's cœfficients $A_1 \dots A_n$ then to add or not the average component. That's why the temporal instant where we add the average component doesn't mind. The average component only change the continuous part of the signal. And this continuous component can be created before the dynamic part exists, because in any case, the temporal signal will be constructed and will exist only when the delayed dynamic part arrives.

The tempoal signal can be separate in its continuous value and its dynamic value. Writing:

$$f(t) = A_0 + \sum_{n\neq 0} A_n cos\left(n2\pi\frac{t}{T}\right) + B_n sin\left(n2\pi\frac{t}{T}\right) \tag{33}$$

we can always define:

$$f_{DC} = A_0 \tag{34}$$

which is the continuous part of f, and

$$\tilde{f}(t) = \sum_{n\neq 0} A_n cos\left(n2\pi\frac{t}{T}\right) + B_n sin\left(n2\pi\frac{t}{T}\right) \tag{35}$$

NGD circuit with line analysis

The two referentials previously described in the NGD circuit given Fig. 7 communicate by exchanging delayed signals. We have seen that the propagation speed in the line is infinite

when the frequency tends to zero. This is completely coherent with the spectrum Independence versus the average value.

Let's try to write this mathematically. We can take Fourier's transform of the source signal $e(t) = \tilde{e}(t) + e_{DC}$. We consider a simple circuit made of two meshes and with the complete fundamental tensor ζ defined by:

$$\zeta = \begin{bmatrix} R_1 + L_1 s & 0 \\ e^{-\tau s} & R_2 + L_2 s \end{bmatrix} \tag{36}$$

To simplify the analysis we consider a single delayed coupling function going from the input to the output. Each mesh belongs to a separate referential. Our circuit is represented by the equation:

$$\begin{bmatrix} e(t) \\ 0 \end{bmatrix} = \begin{bmatrix} R_1 + L_1 \frac{d}{dt} & 0 \\ \delta_\tau & R_2 + L_2 \frac{d}{dt} \end{bmatrix} \begin{bmatrix} J^1(t) \\ J^2(t) \end{bmatrix} \tag{37}$$

We can explore the DC side of this equation:

$$\begin{bmatrix} e_{DC} \\ 0 \end{bmatrix} = \begin{bmatrix} R_1 & 0 \\ 1 & R_2 \end{bmatrix} \begin{bmatrix} J^1_{DC} \\ J^2_{DC} \end{bmatrix} \tag{38}$$

and its dynamic side:

$$\begin{bmatrix} \tilde{e}(s) \\ 0 \end{bmatrix} = \begin{bmatrix} R_1 + L_1 s & 0 \\ e^{-\tau s} & R_2 + L_2 s \end{bmatrix} \begin{bmatrix} \tilde{J}^1 \\ \tilde{J}^2 \end{bmatrix} \tag{39}$$

The solution of the system (38) can be solved independently of the time and it doesn't include the delay function $exp(-\tau s)$, while the solution of the system (39) depends on time. $e(t)$ cannot exist without $\tilde{e}(t)$. Or more accurately speaking, e_{DC} can exist instantaneously but we cannot perceive it. From the moment we make a measurement, we create a dynamic signal or interaction and so, we understand that it is in practice impossible to acquire the continuous signal without a dynamic signal.

In our experience, the continuous component arrives immediately on the normalization amplifier. But if we focus on the start of the signal, as small as it is, we see that it arrives first (Fig.

9 and 10). Then, this advance seems negligible because the amplifier immediately creates the dynamic signal normalized which is many more steep than the original signal. This difference of stiffness gives at lower frequencies a temporal advance of the normalized signal on the original one. As the signal coming from these low frequencies is many more high than the signal coming from the high frequencies, the whole signal seems to go faster than the light speed.

References

1. Garrett and D. E. McGumber, "Propagation of a Gaussian light pulse through an anomalous dispersion medium," Phys. Rev. A, Vol. 1, 1970

2. S. Chu and S. Wong, "Linear Pulse Propagation in an Absorbing Medium," Phys. Rev. Lett., 48, 11, 1982, pp. 738-741.

3. B. Ségard and B. Macke, Observation of negative velocity pulse propagation, Phys. Lett. 109A, 213 (1985).

4. B. Macke, B. Ségard, and F. Wielonsky, Optimal superluminal systems, Phys. Rev. E 72, 035601(R) (2005).

5. B. Ségard and B. Macke, "Two-pulse interference and superluminality," Optics Communications 281 (2008) 12–17.

6. B. Macke and B. Ségard, Propagation of light-pulses at a negative group-velocity, Eur. Phys. J. D 23, 125 (2003).

7. B. Ségard and B. Macke, "On-resonance material fast light," PHYSICAL REVIEW A 97, 063830 (2018)

8. M. W. Mitchell, and R. Y. Chiao, “Negative group delay and ”fronts” in a causal system: An experiment with very low frequency bandpass amplifiers,” Phys. Lett. A, vol. 230, no. 3-4, pp. 133-138, June 1997.

9. M. W. Mitchell and R.Y. Chiao, “Causality and Negative Group-delays in a Simple Bandpass Amplifier,” Am. J. Phys., vol. 66, 1998, pp. 14-19.

10. M. W. Mitchell and R. Y. Chiao, “Negative Group-delay and ‘Fronts’ in a Causal Systems: An Experiment with Very Low Frequency Bandpass Amplifiers,” Phys. Lett. A, vol. 230, Jun. 1997, pp. 133-138.

11. T. Nakanishi, K. Sugiyama and M. Kitano, “Demonstration of Negative Group-delays in a Simple Electronic Circuit,” Am. J. Phys., vol. 70, no. 11, 2002, pp. 1117-1121.

12. M. Kitano, T. Nakanishi and K. Sugiyama, “Negative Group-delay and Superluminal Propagation: An Electronic Circuit Approach,” IEEE J. Sel. Top. in Quantum Electron., vol. 9, no. 1, Feb. 2003, pp. 43-51.

13. J. N. Munday and R. H. Henderson, “Superluminal Time Advance of a Complex Audio Signal,” Appl. Phys. Lett., vol. 85, July 2004, pp. 503-504.

14. B. Ravelo, “Demonstration of negative signal delay with short-duration transient pulse”, Eur. Phys. J. Appl. Phys. (EPJAP), Vol. 55 (10103), 2011, pp. 1-8.

15. B. Ravelo, “Methodology of elementary negative group delay active topologies identification”, IET Circuits Devices Syst. (CDS), Vol. 7, No. 3, May 2013, pp. 105-113.

16. B. Ravelo, “Investigation on microwave negative group delay circuit”, Electromagnetics, Vol. 31, No. 8, Nov. 2011, pp. 537-549.

17. B. Ravelo, “Baseband NGD circuit with RF amplifier”, Electronic Letters, Vol. 47, No. 13, June 2011, pp. 752-754.

18. Sommerfeld, Lectures on Theoretical Physics, Optics. Academic Press Inc. US, 1954

19. L. Brillouin, Wave Propagation in Periodic Structures, McGraw-Hill, New York, 1946

20. L. Brillouin, Wave propagation and group velocity, Academic Press, New York, 1960

21. V. Veselago, Soviet Physics Uspekhi, Vol. 10, No. 4, 1968

22. J. B. Pendry, ”Negative refraction makes a perfect lens,” Phys. Rev. Lett., Vol. 85, 2000

23. D. R. Smith et al., ”Loop-wire for investigating plasmons at microwave frequencies,” Appl. Phys. Lett., Vol. 75, No. 10, Sept. 1999

24. D. R. Smith et al., ”Composite medium with simultaneously negative permittivity and permeability,” Phys. Rev. Lett., Vol. 84, May 2000

25. B. Ravelo, “Similitude between the NGD function and filter gain behaviours”, Int. J. Circ. Theor. Appl., Vol. 42, No. 10, Oct. 2014, pp. 1016–1032.

26. B. Ravelo, “On the low-pass, high-pass, bandpass and stop-band NGD RF passive circuits”, URSI Radio Science Bulletin, Vol. 2017, No. 363, Dec. 2017, pp. 10-27.

27. B. Ravelo, “First-order low-pass negative group delay passive topology”, Electronics Letters, Vol. 52, No. 2, Jan. 2016, pp. 124–126.

28. B. Ravelo, F. Wan and J. Ge, “Anticipating Actuator Arbitrary Action with a Low-Pass Negative Group Delay Function,” IEEE Transactions on Industrial Electronics, Vol. 68, No. 1, Jan. 2021, pp. 694-702.

29. B. Ravelo, “High-Pass Negative Group Delay RC-Network Impedance”, IEEE Transactions on Circuits and Systems II: Express Briefs, Vol. 64, No. 9, Sept. 2017, pp. 1052-1056.

30. B. Ravelo, S. Ngoho, G. Fontgalland, L. Rajaoarisoa, W. Rahajandraibe, R. Vauché, Z. Xu, F. Wan, J. Ge, and S. Lalléchère, “Original Theory of NGD Low Pass-High Pass Composite Function for Designing Inductorless BP NGD Lumped Circuit,” IEEE Access, Vol. 8, No. 1, Oct. 2020, pp. 192951-192964.

31. B. Ravelo, N. Li, F. Wan and J. Feng, “All-Pass Negative Group Delay Function with Transmission Line Feedback Topology,” IEEE Access, Vol. 7, No. 1, Dec. 2019, pp. 155711-155723.

32. B. Ravelo, “Distributed NGD active circuit for RF-microwave communication”, Int. J. Electron. Commun., Vol. 68, No. 4, Apr. 2014, pp. 282-290.

33. B. Ravelo, “Recovery of Microwave-Digital Signal Integrity with NGD Circuits”, Photonics and Optoelectronics (PO), Vol. 2, No. 1, Jan. 2013, pp. 8-16.

34. B. Ravelo, S. Lalléchère, A. Thakur, A. Saini and P. Thakur, “Theory and circuit modelling of baseband and modulated signal delay compensations with low- and band-pass NGD effects”, Int. J. Electron. Commun. (AEÜ), Vol. 70, No. 9, Sept. 2016, pp. 1122–1127.

35. B. Ravelo, W. Rahajandraibe, Y. Gan, F. Wan, N. M. Murad and A. Douyère, “Reconstruction Technique of Distorted Sensor Signals with Low-Pass NGD Function,” IEEE Access, Vol. 8, No. 1, Dec. 2020, pp. 92182-92195.

36. B. Ravelo, “Investigation on the microwave pulse signal compression with NGD circuit”, Progress In Electromagnetics Research (PIER) C, Vol. 20, 2011, pp. 155-171.

37. B. Ravelo, F. Wan, J. Nebhen, W. Rahajandraibe, and S. Lalléchère, “Resonance Effect Reduction with Bandpass Negative Group Delay Fully Passive Function”, IEEE Transactions on Circuits and Systems II: Express Briefs, Vol. 68, No. 7, July 2021, pp. 2364-2368.

38. B. Ravelo, S. Lalléchère, W. Rahajandraibe, and F. Wan, “Electromagnetic Cavity Resonance Equalization with Bandpass Negative Group Delay,” IEEE Transactions on Electromagnetic Compatibility, Vol. 63, No. 4, Aug. 2021, pp. 1248-1257.

39. Philippe A. Martin, and François Rothen, Problèmes à N-corps et champs quantiques, Presses polytechniques Romandes, Lausanne, 1990.